

Supporting Information for
**Efficient construction of hard carbon through hydrothermal
carbon coating strategy toward enhanced sodium-ion storage
performance**

Wenbin Jian¹, Xueqing Qiu^{1,2,3,}, Junjun Yao¹, Lei Zhong¹, Fangbao Fu^{1,2,3}, Xihong Zu^{1,2,3}
and Wenli Zhang^{1,2,3,*}*

¹School of Chemical Engineering and Light Industry, and School of Advanced Manufacturing, Guangdong University of Technology (GDUT), 100 Waihuan Xi Road, Panyu District, Guangzhou 510006, China.

²Guangdong Provincial Laboratory of Chemistry and Fine Chemical Engineering Jieyang Center, Jieyang, 515200, China.

³Guangdong Basic Research Center of Excellence for Ecological Security and Green Development, Guangdong University of Technology, Guangzhou, 510006, China

1. Supporting Experimental Section

1.1 Materials

Alkali lignin (AL) were purchased from Longlive Biotechnology (Shandong province, China). Glucose was purchased from Aladdin Chem. Sodium carboxymethylcellulose (CMC-Na), sodium hexafluorophosphate (NaPF_6), 1,2-Dimethoxyethane (DME), and carbon black were purchased from Guangdong Canrd New Energy Technology Co., Ltd. All other chemical reagents were used without further purification.

1.2 Preparation of material

1.2.1 Preparation of porous carbon

10 g AL was pre-carbonized at 400 °C in air, and the carbonized product was ball-milled for 5 min. The carbon yield at this stage was 63.4%. The carbon material obtained at 400 °C was then activated by steam to prepare lignin-derived porous carbon (PC). The carbon material obtained at 400 °C was placed in a tube furnace and heated to 900 °C under a nitrogen atmosphere. Then steam was introduced by adding water drops into the tube furnace. The water drop flow rate was 3.5 mL min⁻¹. Steam activation lasted for 3 h. Subsequently, water drop addition was stopped, and the sample was cooled to room temperature.

1.2.2 Preparation of hard carbon by coating porous carbon using melting, pyrolysis, and carbonization of glucose

Glucose and PC were ball-milled in a pendulum ball milling jar for 5 min. The mass ratios of glucose to PC were 0.5:1, 1:1, and 2:1. The solid mixture after ball milling was placed in a tube furnace and heated at a rate of 2 °C min⁻¹ under a nitrogen atmosphere to 200 °C, where it was held for 2 h. Next, the temperature was increased at a rate of 5 °C min⁻¹ to 1300 °C,

where it was held for 4 h. The obtained hard carbons were denoted as PC-G-0.5-1-1300, PC-G-1-1-1300, and PC-G-1-2-1300, respectively.

1.2.3 Preparation of hard carbon through coating porous carbon using a hydrothermal glucose strategy

Glucose, PC, and water were added to a hydrothermal reactor at predetermined ratios and stirred until glucose was completely dissolved. The mass ratios of glucose, PC, and water were 0.25:1:0.25, 0.5:1:0.5, and 1:1:1, respectively. After homogeneous mixing, the reactor was placed in an 180 °C oven for 5 h. After the end of the reaction, the product was transferred to an 80 °C drying oven to remove the inner moisture. The dried solid samples were then placed in a tube furnace for high-temperature heat treatment under a nitrogen atmosphere. The temperature was first raised to 200°C at a heating rate of 2°C min⁻¹ and held for 2 h, followed by heating to 1300°C at 5°C min⁻¹ for 4 h. The obtained hard carbon materials were denoted as PC-HG-0.25-1-1300, PC-HG-1-0.5-1300, and PC-HG-1-1-1300, respectively.

1.3 Electrode preparation

The HC electrodes were prepared by mixing the HC samples with carbon black and CMC-Na at a weight ratio of 8:1:1 in ultrapure water solvents (mechanically mixed for at least 1 h) and casting on Cu foil with the blade coating technique. After drying at 80 °C under vacuum for 12 h, the electrodes were cut into discs with a diameter of 12 mm. The mass loadings of electrodes were around 1.5 mg cm⁻². Half cells (CR2032) were assembled with sodium metal foil (99.8%, Aladdin, China) as the counter/reference electrode, a glass-fiber separator (Whatman), and 1 M NaPF₆ dissolved in DME as an electrolyte. All the assembling operations were conducted in the argon-filled glove box.

1.4 Material characterization

1.4.1 Structural analysis

X-ray diffraction patterns were collected on a D8 Advance X-ray diffractometer (XRD, Bruker, Germany) with Cu K α radiation ($\lambda = 1.5406 \text{ \AA}$). The defect degrees of HCs were characterized by the LabRAM HR Evolution microconfocal Raman spectrometer (Raman, HORIBA Jobin Yvon, France). The thermosetting analysis of samples were characterized by differential scanning calorimetry (DSC, DSC8000, Perkin Elmer). The thermogravimetric analysis of samples were performed by thermogravimetric analysis (TGA, TGA 4000, Perkin Elmer). The small-angle X-ray scattering (SAXS) and wide-angle X-ray scattering (WAXS) were collected on the BL19U2 of the Shanghai Synchrotron Radiation Facility. The specific surface areas and open pore diameters were measured at 77 K using ASAP 2460 N₂ adsorption/desorption (Micromeritics, USA). The SAXS data were analyzed using the SasView 4.2.2¹. The semi-empirical Teubner-Strey model with SAXS was used to analyze the pore structure of HC. The morphologies of the samples were investigated by a SU8220 scanning electron microscope (SEM, Hitachi, Japan). A IS50R Fourier transform infrared spectroscopy (FTIR, Thermo Fisher Scientific, USA) was performed on the sample using the KBr pallet method.

1.4.2 Electrochemical tests

The galvanostatic charge/discharge (GCD) tests were conducted on a BTS4008-5V-20mA Neware battery test system (Neware, Shenzhen, China) at room temperature. The cyclic voltammetry (CV) and electrochemical impedance spectroscopy (EIS) measurements were

conducted on a VMP3e and DH7000 electrochemical workstation (Bio-Logic, France, and DongHua Test, China).

There is a power-law relationship between the scan rate (ν) and the peak current (I) in CV:

$$I = a\nu^b \quad (\text{S1})$$

The b -value is calculated by converting the equation (S2) to

$$\log I = b \log \nu + \log a \quad (\text{S2})$$

where i is the peak current, mA; ν is the scan rate, mV s⁻¹; a and b are adjustable values.

The diffusion coefficient of Na⁺ ions was determined using the galvanostatic interval titration technique (GITT). Before testing the GITT, the sample was cycled three times at a current density of 0.05 A g⁻¹. The galvanostatic section of the GITT was conducted at a current of 0.05 A g⁻¹ for 5 min, followed by a relaxation section for 2 h. The diffusion coefficient of Na⁺ ions was calculated using the following equation²:

$$D_{Na^+} = \frac{4}{\pi} \left(\frac{V_M}{I_0 F S} \right)^2 \left(\frac{dE_{ep}/dx}{dE/dt^{1/2}} \right)^2 ; t \ll L^2/D \quad (\text{S3})$$

where, D_{Na^+} is the diffusion coefficient of Na⁺ ions (m² s⁻¹), I_0 is the current during the galvanostatic phase of GITT (A), V_m is the molar volume of the active material (m³ mol⁻¹), F is the Faraday constant (96485 C mol⁻¹), S is the electrode area (contact area between carbon and electrolyte, m²), dE_{ep}/dx is the slope of the equilibrium potential versus sodium content curve during the constant current phase (V), $dE/dt^{1/2}$ is the slope deduced from E versus $t^{1/2}$ during the relaxation phase (V s^{-1/2}), and L is the diffusion length (m).

Note S1. Detailed data analysis of XRD

The interlayer spacing of (002) and (100) crystalline planes is calculated by the Bragg equation:

$$2d\sin\theta = n\lambda \quad (\text{S4})$$

where d is interlayer spacing, θ is half of peak center 2θ , and λ is the wavelength of the X-ray (0.154 nm).

The crystalline length (L_a) and thickness (L_c) of HC could be calculated by the Scherrer equations:

$$L(\text{nm}) = \frac{K\lambda}{\beta \cos\theta} \quad (\text{S5})$$

where K values of 1.84 and 0.90 are for the (100) and (002) peaks of the carbon materials, respectively, and β is the full-width half maximum (FWHM) of the XRD peak. The FWHM of L_c and L_a is calculated using the FWHM of the diffraction peak of the (002) crystalline plane and the (100) crystalline plane, respectively.

The number of graphene layer stacks (N) is calculated by the following equation:

$$N = \frac{L_c}{d_{002}} + 1 \quad (\text{S6})$$

Note S2. Absolute intensity calibration of SAXS data³

HCs are composed of randomly arranged stacked graphene nanodomains and abundant nanopores. HCs exhibit pore-scattering shoulders in the range of scattering vectors Q from 0.08 to 0.8 \AA^{-1} . The pore size information of HC could be obtained by fitting the SAXS curve of HC. If it is necessary to calculate the pore volume fraction of HC by SAXS, the absolute intensity of the SAXS signal must be calibrated. We used glassy carbon as a standard SAXS sample (NIST SRM 3600, SN: D28) to calibrate the scattering intensity of HC.

The HC sample is a powder sample and the glassy carbon is a bulk sample. There is a gap between the powder samples. And the thickness between HC and glassy carbon is not consistent. Therefore, transmission and thickness calibration of HC samples are performed.

$$I_{d,T}(Q) = \frac{I_{HC}(Q) \times T_{HC}}{d_{HC}} \quad (S7)$$

$$SF = \frac{I_{abs,GC}(Q)}{I_{GC}(Q)} \quad (S8)$$

$$I_{abs,HC}(Q) = \frac{I_{d,T}(Q) \times SF \times d_{GC}}{T_{GC}} \quad (S9)$$

Where $I_{d,T}(Q)$ is the normalized intensity for the thickness (d_{HC}) and the transmission coefficient (T_{HC}) of the HC sample. SF is the calibration factor. $I_{abs,GC}(Q)$ and $I_{GC}(Q)$ are the absolute and experimental intensities, respectively. $I_{abs,HC}$ is the absolute intensity of the HC. d_{GC} is the thickness of the glassy carbon, and T_{GC} is the transmission coefficient of the glassy carbon.

$I_{abs,HC}(Q)$ is the volumetric scattering cross-section of the sample with units of cm^{-1} . The specific mass scattering cross-section $I^{\text{cm}^2 \text{ g}^{-1}}$ can be obtained by normalizing the volumetric scattering cross-section $I^{\text{cm}^{-1}}$ by effective bulk density ρ_{eff} . The ρ_{eff} of a powder sample at the

illuminated spot is determined based on the transmission of the sample, which takes into account the specific attenuation factor for carbon μ/ρ^4 :

$$I^{\text{cm}^2 \text{ g}^{-1}}(\text{Q}) = \frac{I^{\text{cm}^{-1}(\text{Q})}}{\rho_{\text{eff}}} \quad (\text{S10})$$

$$\rho_{\text{eff}} = \frac{\ln T_{\text{HC}}}{\mu/\rho \cdot d_{\text{HC}}} \quad (\text{S11})$$

Here, μ/ρ is the X-ray mass attenuation coefficient of the sample. The $\mu/\rho = 4.51$ and $1.37 \text{ cm}^2 \text{ g}^{-1}$ have been determined by interpolation of the NIST data base at the photon energy corresponding to Cu K- α (8.04 keV) and synchrotron radiation source (12.00 keV), respectively.

Note S3. Detailed data analysis process of SAXS

The SAXS curves at scattering vectors (Q) lower than 1 \AA^{-1} can be divided into three parts: (1) a slope in Q^{-n} at Q lower than 0.08 \AA^{-1} , corresponding to Porod's law for scattering from macroscopic sharp surfaces of powder grains (I_{Porod}); (2) the scattering from micropores in the 0.08 to 1 \AA^{-1} Q range (I_{mp}); (3) the background scattering signal ($I_{\text{backgrounds}}$):

$$I^{\text{SAXS}}(Q) = I_{\text{Porod}} + I_{\text{mp}} + I_{\text{backgrounds}} \quad (\text{S12})$$

The pore structure of HC is analyzed by the semi-empirical Teubner-Strey model⁴:

$$I_{\text{mp}} = I_0 \frac{1}{1 + C_1 Q^2 + C_2 Q^4} \quad (\text{S13})$$

Here I_0 , C_1 and C_2 are obtained by adjusting the following equations:

$$I_0 = \frac{8\pi}{\rho_{\text{struc}}} \phi (\Delta SLD)^2 \frac{\xi^3}{\left(1 + \left(\frac{2\pi\xi}{d}\right)^2\right)^2} \quad (\text{S14})$$

$$d = 2\pi \left[\frac{1}{2} C_2^{-\frac{1}{2}} - \frac{C_1}{4C_2} \right]^{-\frac{1}{2}} \quad (\text{S15})$$

$$\xi = 2\pi \left[\frac{1}{2} C_2^{-\frac{1}{2}} + \frac{C_1}{4C_2} \right]^{-\frac{1}{2}} \quad (\text{S16})$$

Where ρ_{struc} is the structural density, SLD is the contrast of scattering length density. The SLD of the carbon material is calculated by the software SasView 4.2.2. The SLD of the pores is 0. ΔSLD is equal to the SLD of the carbon material minus the SLD of the pore. d is the pore-pore distance, and ξ is the correlation length that limits the extension of the order. The d and ξ are finally obtained by fitting SasView 4.2.2.

The carbon material ρ_{struc} is obtained by the equation:

$$\rho_{\text{struc}} = \rho_{\text{graphite}} \frac{d_{002}^{\text{graphite}}}{d_{002}} \left(\frac{d_{100}^{\text{graphite}}}{d_{100}} \right)^2 \quad (\text{S17})$$

The average pore size D could be calculated by the following equation:

$$D = 2\sqrt{5C_1} \quad (\text{S18})$$

A parameter f_a , called “amphiphilic factor” for microemulsions³, could be considered as the connectivity level of HC pore:

$$f_a = \frac{C_1}{2\sqrt{C_2}} \quad (\text{S19})$$

A larger value of f_a indicates that the pores are more disordered and connected.

The specific surface area of nanopores ($S_{nanopore}$) is evaluated using the following formula⁴:

$$S_{nanopore} = \frac{I_0}{C_2 2\pi(\Delta SLD)^2} \quad (\text{S20})$$

Note S4. Detailed data analysis process of galvanostatic intermittent titration technique (GITT)

GITT measurements for the anodes consist of a series of current pulses applied at 0.1 A g⁻¹, each followed by a 2 h relaxation period. Due to the inevitable decomposition of electrolyte and formation of SEI film, GITT are testing at the third cycles. Generally, Fick's second law⁵ (Eq. S21) is used to describe the unsteady diffusion process.

$$D_{Na^+} = \frac{4}{\pi\tau} \left(\frac{m_B V_M}{S F M_B} \right)^2 \left(\frac{\Delta E_s}{\Delta E_\tau} \right)^2 \quad (S21)$$

The calculation of ΔE_s (steady-state potential change after relaxation) and ΔE_τ (potential change during constant current stage), which involves differentiating the potential time curve to obtain the potential change per unit time, is the core basis for subsequent diffusion coefficient calculations; τ is the constant current charge discharge time, M_B is the mass of the active material, V_M is the molar volume, S is the electrode specific surface area, F is the Faraday constant, and M_B is the molar mass.

The reason for choosing the GITT differential method in this study is that it can reflect the sodium-ion diffusion behavior of hard carbon anodes in situ during actual charge and discharge processes, which is highly compatible with the research core of this article on the influence of pore structure regulation on sodium ion transport kinetics.

Detailed calculation steps: Perform constant current charging/discharging on the electrode (using 0.05 A g⁻¹ in this study) for a duration of $\tau=7200$ s. Stop the constant current and allow the electrode to relax to steady state (potential change < 0.001 V h⁻¹), record the potential ΔE_s before and after relaxation and the potential ΔE_τ during the constant current stage. Differentiate the potential time curves of different potential segments and calculate the $\Delta E_s/\Delta E_\tau$ of each potential segment. Substitute the above parameters into the classical GITT formula to calculate the D_{Na^+} of each potential segment. Analyze the variation patterns of D_{Na^+} under different reaction mechanisms by dividing the sodium storage potential range of hard carbon.

2. Supporting Tables

Table S1 Crystalline structure parameters of samples calculated via XRD measurements

Sample	d_{002} (nm)	L_c (nm)	N	d_{100} (nm)	L_a (nm)	ρ_{struct} (g cm ⁻³)
PC-G-1300	0.387	1.10	3.86	0.206	5.24	2.15
PC-HG-1300	0.387	1.19	4.08	0.206	6.27	2.15
PC-G-200	0.425	1.09	3.56	0.202	5.19	2.03
PC-G-600	0.379	1.08	3.85	0.206	5.19	2.19
PC-G-900	0.377	1.12	3.98	0.207	5.08	2.18
PC-HG	0.389	1.01	3.59	0.204	4.61	2.17
PC-HG-200	0.400	0.96	3.41	0.205	4.94	2.09
PC-HG-600	0.397	0.94	3.38	0.206	4.87	2.09
PC-HG-900	0.379	1.09	3.87	0.206	4.82	2.19

Note:

d_{002} : interlayer spacing of the (002) crystalline plane

L_c : crystalline thickness

L_a : crystalline length

d_{100} : interlayer spacing of the (100) crystalline plane

N: the number of graphene layer stacks

ρ_{struct} : structural density

Table S2 Morphological parameters of the nanopores deduced from SAXS patterns based on the Teubner-Strey model.

Sample	ρ_{struct} (g cm⁻³)	ΔSLD (*10⁻⁶ Å⁻²)	d (nm)	ξ (nm)	D (nm)
PC-HG-1300	2.15	18.3	4.36	0.47	1.50
PC-G-1300	2.15	18.3	5.26	0.57	1.80
PC-HG	2.17	18.4	3.06	0.42	0.76
PC-HG-200	2.09	17.7	3.18	0.44	0.75
PC-HG-600	2.09	17.7	4.31	0.57	1.17
PC-HG-900	2.19	18.6	4.46	0.58	1.27
PC-G-600	2.19	18.6	6.63	0.96	1.36
PC-G-900	2.18	18.5	5.16	0.62	1.64

Note:

ρ_{struct} : structural density

SLD: scattering length density

d: pore-pore distance

ξ : a correlation length that limits the extension of the order

D: pore diameter

Table S3 Pore structure parameters of the nanopores deduced from SAXS patterns based on the Teubner-Strey model.

Sample	f_a	micropore volume fraction ϕ	pore volume (cm³ g⁻¹)	pore number (*10⁻³ nm⁻³)	nanopore specific surface area (m² g⁻¹)
PC-HG-1300	0.37	31.6%	0.215	177.9	1286
PC-G-1300	0.36	28.8%	0.188	93.9	939
PC-HG	0.14	11.3%	0.059	497.0	699
PC-HG-200	0.13	12.3%	0.067	547.7	801
PC-HG-600	0.18	20.2%	0.121	240.3	932
PC-HG-900	0.20	25.6%	0.157	240.3	1115.8
PC-G-600	0.09	19.8%	0.113	150.2	746
PC-G-900	0.27	25.1%	0.154	108.7	844

f_a : disorder parameter

3. Supporting Figures

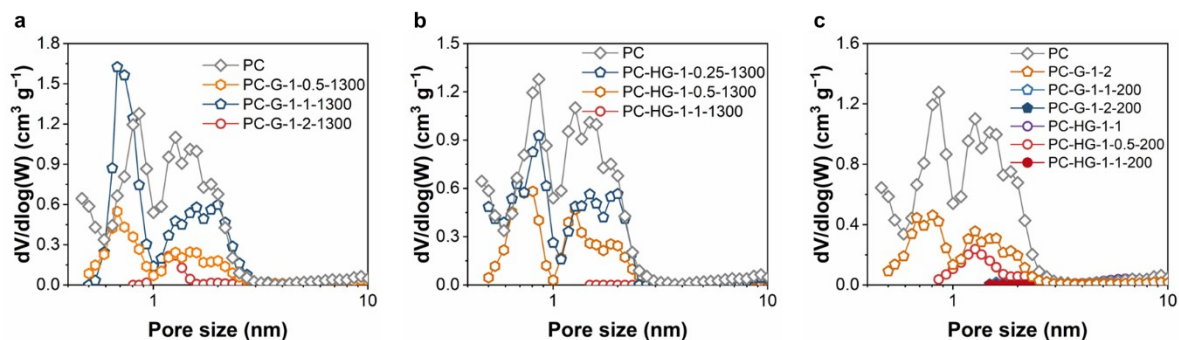


Figure S1. (a) Pore size distribution for PC, PC-G-1-0.5-1300, PC-G-1-1-1300, and PC-G-1-2-1300. (b) Pore size distribution for PC, PC-HG-1-0.25-1300, PC-HG-1-0.5-1300, and PC-HG-1-1-1300. (c) Pore size distribution of PC, PC-G-1-2, PC-G-1-1-200, PC-G-1-2-200, PC-HG-1-1, PC-HG-1-0.5-200, and PC-HG-1-1-200.

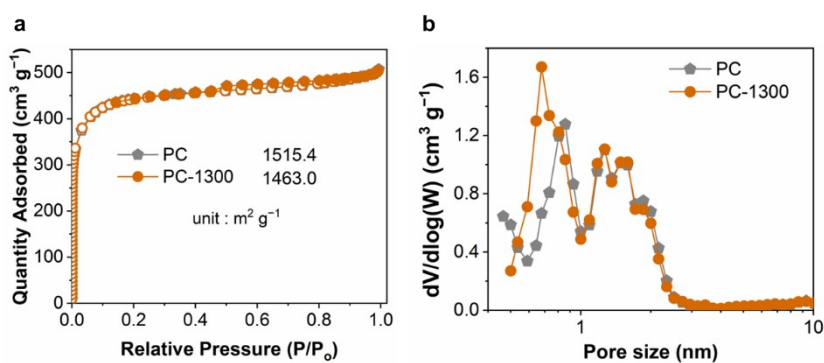


Figure S2. (a) Nitrogen adsorption/desorption isotherms of PC and PC-1300. (b) Pore size distribution of PC and PC-1300.

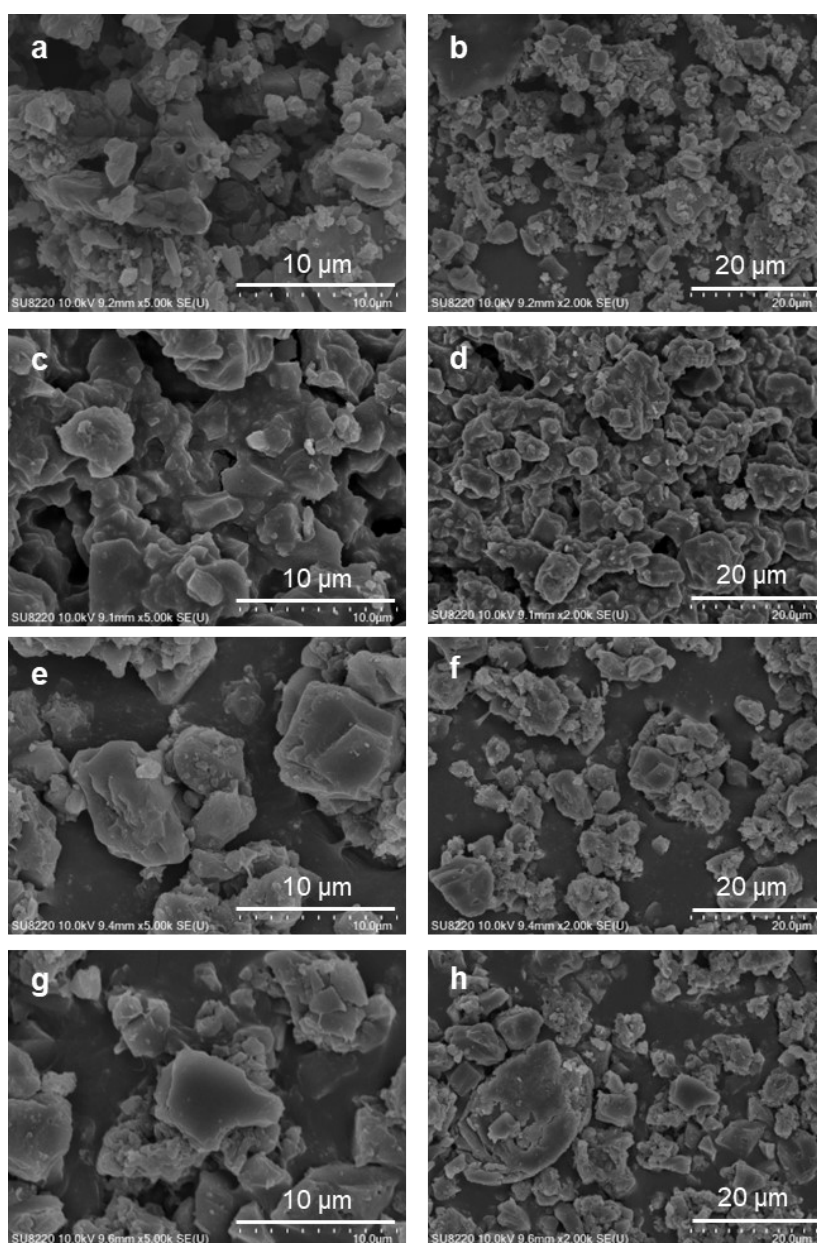


Figure S3. SEM images of (a, b) PC-G-1-2, (c, d) PC-G-1-2-200, (e, f) PC-G-1-2-600, and (g, h) PC-G-1-2-1300.

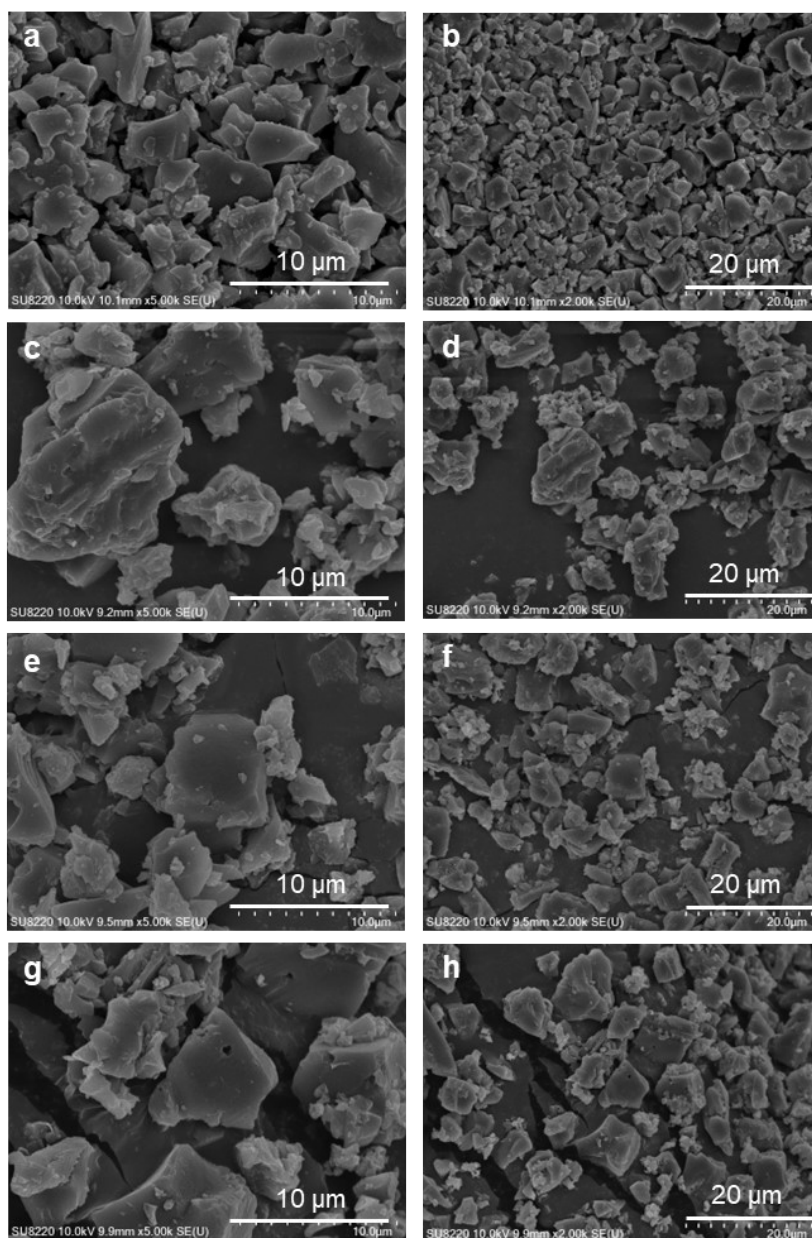


Figure S4. SEM images of (a, b) PC-HG-1-1, (c, d) PC-HG-1-1-200, (e, f) PC-HG-1-1-600, and (g, h) PC-HG-1-1-1300.

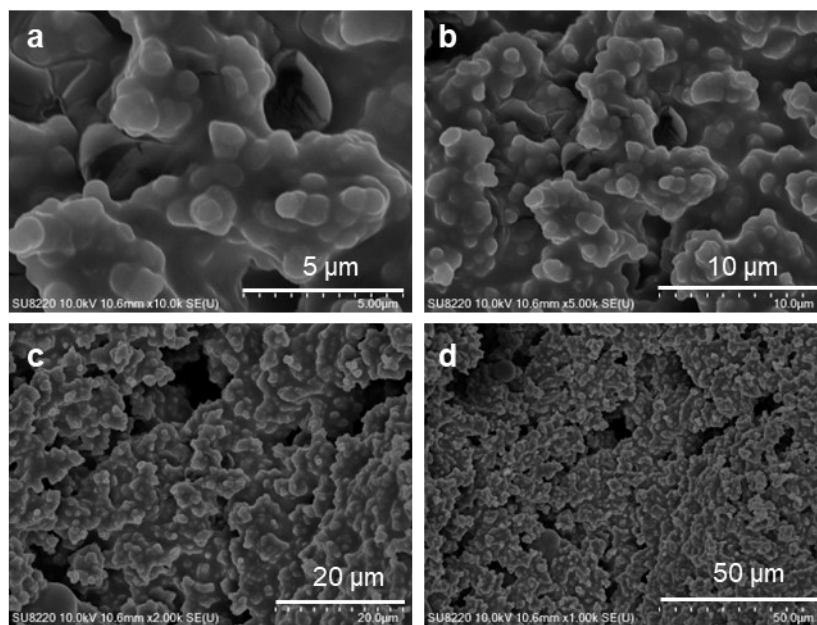


Figure S5. (a-d) SEM images of hydrothermal glucose.

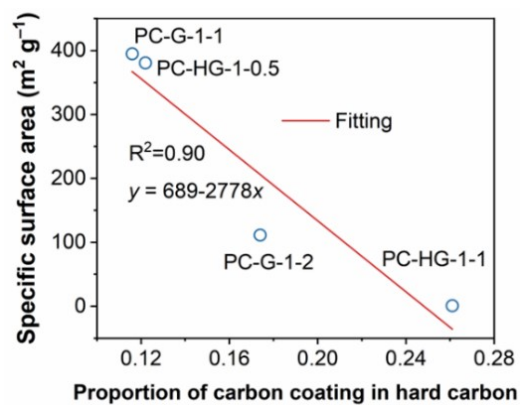


Figure S6. Relationship between proportion of carbon coating in HC and specific surface area.

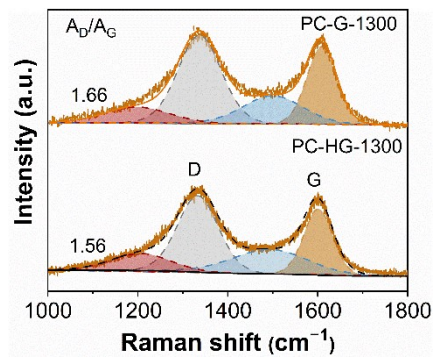


Figure S7. Raman spectrum of PC-G-1300 and PC-HC-1300.

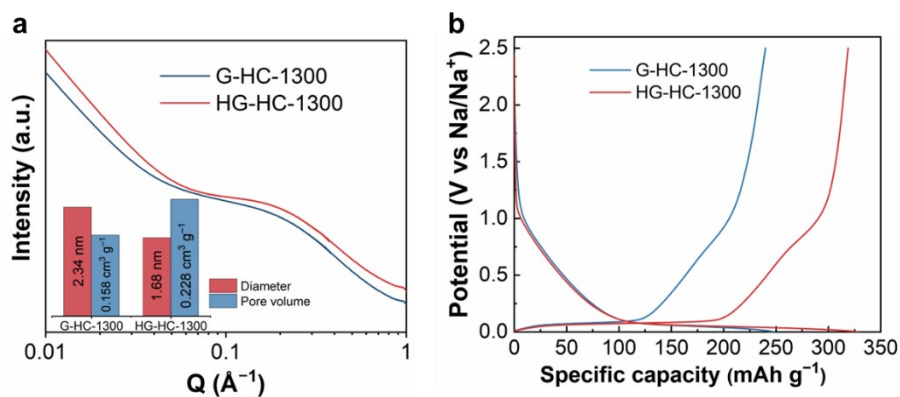


Figure S8. SAXS patterns and GCD curve at 0.05 A g^{-1} for G-HC-1300 and HG-HC-1300.

Note: G-HC-1300 was prepared by directly heat-treating glucose at 1300°C for 2 hours. 1 g of glucose was dissolved in 1 g of water to form a high-concentration glucose aqueous solution. The glucose aqueous solution was placed in a hydrothermal reactor and maintained at 180°C for 5 hours. After the end of the reaction, the product was transferred to an 80°C drying oven to remove the inner moisture. The dried solid samples were then placed in a tube furnace for high-temperature heat treatment under a nitrogen atmosphere. The temperature was first raised to 200°C at a heating rate of 2°C min^{-1} and held for 2 h, followed by heating to 1300°C at 5°C min^{-1} for 4 h. The hard carbon obtained after hydrothermal and high-temperature heat treatment was denoted as HG-HC-1300.

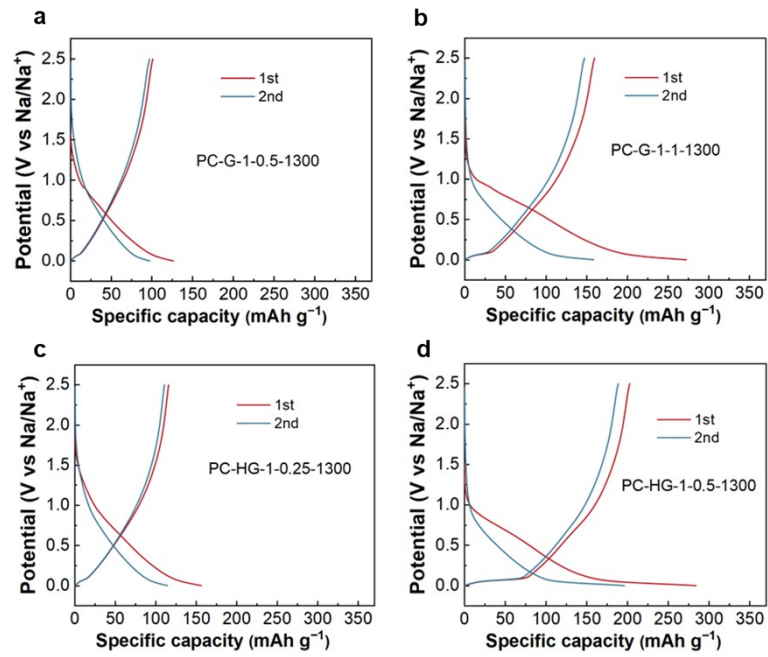


Figure S9. The 1st and 2nd GCD curves for PC-G-1-0.5-1300, PC-G-1-1-1300, PC-HG-1-0.25-1300, and PC-HG-1-0.5-1300 at 0.05 A g⁻¹.

Reference

1. Doucet, M.; Cho, J.; Alina, G.; Bakker, J.; Bouwman, W.; Butler, P.; Campbell, K.; Gonzales, M.; Heenan, R.; Jackson, A., *Zenodo* **2019**, 1412041.
2. Aniskevich, Y.; Yu, J. H.; Kim, J. Y.; Komaba, S.; Myung, S. T., *Advanced Energy Materials* **2024**, *14* (18), 2304300.
3. Zeng, J.; Bian, F.; Wang, J.; Li, X.; Wang, Y.; Tian, F.; Zhou, P., *Journal of Synchrotron Radiation* **2017**, *24* (2), 509-520.
4. Saurel, D.; Segalini, J.; Jauregui, M.; Pendashteh, A.; Daffos, B.; Simon, P.; Casas-Cabanas, M., *Energy Storage Materials* **2019**, *21*, 162-173.
5. Guo, Z. Y.; Xu, Z.; Xie, F.; Jiang, J. L.; Zheng, K. T.; Alabidun, S.; Crespo-Ribadeneyra, M.; Hu, Y. S.; Au, H.; Titirici, M.-M., *Adv. Mater.* **2023**, *35* (42), 2304091.